molecular pharmaceutics

articles

Profiling Proteasome Activity in Tissue with Fluorescent Probes

Celia R. Berkers,[†,‡] Fijs W. B. van Leeuwen,[†,‡,§] Tom A. Groothuis,[||] Victor Peperzak,[⊥] Erica W. van Tilburg,[†,@] Jannie Borst,[⊥] Jacques J. Neefjes,[||] and Huib Ovaa*[,†]

Divisions of Cellular Biochemistry, Tumor Biology, and Immunology, The Netherlands Cancer Institute, Plesmanlaan 121, 1066 CX Amsterdam, The Netherlands

Received March 2, 2007; Revised Manuscript Received May 10, 2007; Accepted June 14, 2007

Abstract: With proteasome inhibitors in use in the clinic for the treatment of multiple myeloma and with clinical trials in progress investigating the treatment of a variety of hematologic and solid malignancies, accurate methods that allow profiling of proteasome inhibitor specificity and efficacy in patients are in demand. Here, we describe the development, full biochemical validation, and comparison of fluorescent proteasome activity reporters that can be used to profile proteasome activities in living cells with high sensitivity. Seven of the synthesized probes tested label proteasomes in lysates, although the fluorescent dye used affects their specificity. Two differentially labeled probes tested are suitable for studying proteasome activity in living cells by gel-based assays, by confocal laser scanning microscopy, and by flow cytometry. We established methods using these fluorescent reporters to profile proteasome activity in different mouse tissues, carefully avoiding postlysis artifacts, and we show that proteasome subunit activity is regulated in an organ-specific manner. The techniques described here could be used to study in vivo pharmacological properties of proteasome inhibitors.

Keywords: Proteasome; activity profiling; proteasome inhibitor; vinylsulfone; confocal microscopy; ubiquitin

Introduction

The clinical value of proteasome inhibition has recently become evident. The proteasome inhibitor bortezomib[1] is currently used to treat multiple myeloma, while a therapeutic effect on several other (solid) tumors has also been shown.[2] The proteasome is responsible for the degradation of misfolded and redundant proteins[3] as well as a variety of key proteins involved in the regulation of cell proliferation and survival.[4] Proteasome inhibition disrupts these pathways, leading to the suppression of NF-κB activity and stabilization of the tumor suppressor p53,[5] among others. Both suppression of NF-κB activity and p53 stability have been suggested

* To whom correspondence should be addressed: The Netherlands Cancer Institute, Division of Cellular Biochemistry, Plesmanlaan 121, 1066 CX Amsterdam, The Netherlands. Fax: +31205121989. E-mail: h.ovaa@nki.nl.

[†] Division of Cellular Biochemistry.

[‡] These authors contributed equally to this work.

[§] Present address: Division of Diagnostic Oncology, The Netherlands Cancer Institute-Antoni van Leeuwenhoek Hospital, Plesmanlaan 121, 1066 CX Amsterdam, The Netherlands.

[||] Division of Tumor Biology.

[⊥] Division of Immunology.

[@] Present address: Erasmus Medical Center Rotterdam, Department of Nuclear Medicine, 's-Gravendijkwal 230, 3015 CE Rotterdam, The Netherlands.

(1) Hideshima, T.; Richardson, P.; Chauhan, D.; Palombella, V. J.; Elliott, P. J.; Adams, J.; Anderson, K. C. The proteasome inhibitor PS-341 inhibits growth, induces apoptosis, and overcomes drug resistance in human multiple myeloma cells. *Cancer Res.* **2001**, *61*, 3071–3076.

(2) Richardson, P. G.; Mitsiades, C.; Hideshima, T.; Anderson, K. C. Bortezomib: Proteasome inhibition as an effective anticancer therapy. *Annu. Rev. Med.* **2006**, *57*, 33–47.

(3) Etlinger, J. D.; Goldberg, A. L. A soluble ATP-dependent proteolytic system responsible for the degradation of abnormal proteins in reticulocytes. *Proc. Natl. Acad. Sci. U.S.A.* **1977**, *74*, 54–58.

(4) Glickman, M. H.; Ciechanover, A. The ubiquitin-proteasome proteolytic pathway: Destruction for the sake of construction. *Physiol. Rev.* **2002**, *82*, 373–428.

10.1021/mp0700256 CCC: $37.00
Published on Web 08/21/2007

to be at least in part responsible for the observed apoptotic effects.[2,5] Since side effects of bortezomib are substantial and since a response is observed only in a subset of patients,[2] there is an emerging demand for methods for accurately assessing the inhibitory action and efficacy of proteasome inhibitors in clinical subjects. Such a method may allow treatment to be adjusted to individual cases, minimizing side effects and strengthening treatment responses. Next to diagnostic applications, proteasome probes are also likely to advance basic research in proteasome action since this line of research heavily depends on the sensitivity of tools available.

The catalytic activity of the proteasome resides within the 20S core and is provided by three constitutive subunits, termed β1, β2, and β5, and/or their inducible immunoproteasome counterparts β1i, β2i, and β5i. It is widely accepted that immunoproteasome subunits are mainly expressed in lymphoid tissues,[6] e.g., spleen, lymph nodes, and thymus. In addition, it is rapidly becoming apparent that different organs express different ratios of constitutive, immuno, and hybrid proteasomes.[7,8] These proteasome subtypes differ with regard to their activity against (fluorogenic) peptide and protein substrates.[7,8] Consequently, proteasome activity and specificity could be organ-specific.[6,7] This is, however, not experimentally validated and requires sensitive techniques to enable the detection of active subunit compositions.

Three different methods are currently used to monitor proteasome activity: fluorogenic assays,[9,10] small molecule-based activity assays,[11–14] and models based on recombinant reporter proteins.[15–18] Fluorogenic and most small molecule assays cannot be used to probe living cells or tissue, whereas the use of reporter proteins remains confined to genetically altered cells or organisms and thus does not allow profiling of patient material. Recently, we reported the development of the dansylated vinylsulfone-based proteasome inhibitor **2** (Figure 1), which contains an α,β-unsaturated sulfone part that reacts with the γ-hydroxyl of the N-terminal threonine residue of catalytic β-subunits of the proteasome,[19] while the use of antibodies against the dansyl moiety allows the detection of labeled subunits by SDS–PAGE and Western blot analysis. This probe is the first of its kind to profile the specificity of proteasome inhibitors in living cells.[19,20]

Since probe **2** requires Western blotting to produce an activity-based readout, we reasoned that this probe could be further optimized by replacing the environment sensitive and low-quantum yield dansyl fluorophore with high-quantum yield fluorophores. This allows direct scanning of the gel for fluorescence emission for visualization of labeled subunits. We recently showed[14] in an initial report that this concept affords a more reliable and sensitive readout in cell lysates, living cells, and tissue using inhibitor **3**. The use of fluorescent probes allows profiling of large numbers of

(5) Concannon, C. G.; Koehler, B. F.; Reimertz, C.; Murphy, B. M.; Bonner, C.; Thurow, N.; Ward, M. W.; Villunger, A.; Strasser, A.; Kogel, D.; Prehn, J. H. Apoptosis induced by proteasome inhibition in cancer cells: Predominant role of the p53/PUMA pathway. *Oncogene* **2007**, *26*, 1681–1692.

(6) Stohwasser, R.; Standera, S.; Peters, I.; Kloetzel, P. M.; Groettrup, M. Molecular cloning of the mouse proteasome subunits MC14 and MECL-1: Reciprocally regulated tissue expression of interferon-γ-modulated proteasome subunits. *Eur. J. Immunol.* **1997**, *27*, 1182–1187.

(7) Dahlmann, B.; Ruppert, T.; Kuehn, L.; Merforth, S.; Kloetzel, P. M. Different proteasome subtypes in a single tissue exhibit different enzymatic properties. *J. Mol. Biol.* **2000**, *303*, 643–653.

(8) Dahlmann, B.; Ruppert, T.; Kloetzel, P. M.; Kuehn, L. Subtypes of 20S proteasomes from skeletal muscle. *Biochimie* **2001**, *83*, 295–299.

(9) Elliott, P. J.; Soucy, T. A.; Pien, C. S.; Adams, J.; Lightcap, E. S. Assays for proteasome inhibition. *Methods Mol. Med.* **2003**, *85*, 163–172.

(10) Lightcap, E. S.; McCormack, T. A.; Pien, C. S.; Chau, V.; Adams, J.; Elliott, P. J. Proteasome inhibition measurements: Clinical application. *Clin. Chem.* **2000**, *46*, 673–683.

(11) Bogyo, M.; Shin, S.; McMaster, J. S.; Ploegh, H. L. Substrate binding and sequence preference of the proteasome revealed by active-site-directed affinity probes. *Chem. Biol.* **1998**, *5*, 307–320.

(12) Kessler, B. M.; Tortorella, D.; Altun, M.; Kisselev, A. F.; Fiebiger, E.; Hekking, B. G.; Ploegh, H. L.; Overkleeft, H. S. Extended peptide-based inhibitors efficiently target the proteasome and reveal overlapping specificities of the catalytic β-subunits. *Chem. Biol.* **2001**, *8*, 913–929.

(13) Ovaa, H.; van Swieten, P. F.; Kessler, B. M.; Leeuwenburgh, M. A.; Fiebiger, E.; van den Nieuwendijk, A. M. C. H.; Galardy, P. J.; van der Marel, H. L.; Ploegh, H. L.; Overkleeft, H. S. Chemistry in living cells: Detection of active proteasomes by a two-step labeling strategy. *Angew. Chem., Int. Ed.* **2003**, *42*, 3626–3629.

(14) Verdoes, M.; Florea, B. I.; Menendez-Benito, V.; Maynard, C. J.; Witte, M. D.; van der Linden, W. A.; van den Nieuwendijk, A. M.; Hofmann, T.; Berkers, C. R.; van Leeuwen, F. W.; Groothuis, T. A.; Leeuwenburgh, M. A.; Ovaa, H.; Neefjes, J. J.; Filippov, D. V.; van der Marel, G. A.; Dantuma, N. P.; Overkleeft, H. S. A fluorescent broad-spectrum proteasome inhibitor for labeling proteasomes in vitro and in vivo. *Chem. Biol.* **2006**, *13*, 1217–1226.

(15) Dantuma, N. P.; Lindsten, K.; Glas, R.; Jellne, M.; Masucci, M. G. Short-lived green fluorescent proteins for quantifying ubiquitin/proteasome-dependent proteolysis in living cells. *Nat. Biotechnol.* **2000**, *18*, 538–543.

(16) Fiebiger, E.; Story, C.; Ploegh, H. L.; Tortorella, D. Visualization of the ER-to-cytosol dislocation reaction of a type I membrane protein. *EMBO J.* **2002**, *21*, 1041–1053.

(17) Lindsten, K.; Menendez-Benito, V.; Masucci, M. G.; Dantuma, N. P. A transgenic mouse model of the ubiquitin/proteasome system. *Nat. Biotechnol.* **2003**, *21*, 897–902.

(18) Luker, G. D.; Pica, C. M.; Song, J.; Luker, K. E.; Piwnica-Worms, D. Imaging 26S proteasome activity and inhibition in living mice. *Nat. Med.* **2003**, *9*, 969–973.

(19) Berkers, C. R.; Verdoes, M.; Lichtman, E.; Fiebiger, E.; Kessler, B. M.; Anderson, K. C.; Ploegh, H. L.; Ovaa, H.; Galardy, P. J. Activity probe for in vivo profiling of the specificity of proteasome inhibitor bortezomib. *Nat. Methods* **2005**, *2*, 357–362.

(20) Chauhan, D.; Catley, L.; Li, G.; Podar, K.; Hideshima, T.; Velankar, M.; Mitsiades, C.; Mitsiades, N.; Yasui, H.; Letai, A.; Ovaa, H.; Berkers, C.; Nicholson, B.; Chao, T. H.; Neuteboom, S. T.; Richardson, P.; Palladino, M. A.; Anderson, K. C. A novel orally active proteasome inhibitor induces apoptosis in multiple myeloma cells with mechanisms distinct from Bortezomib. *Cancer Cell* **2005**, *8*, 407–419.

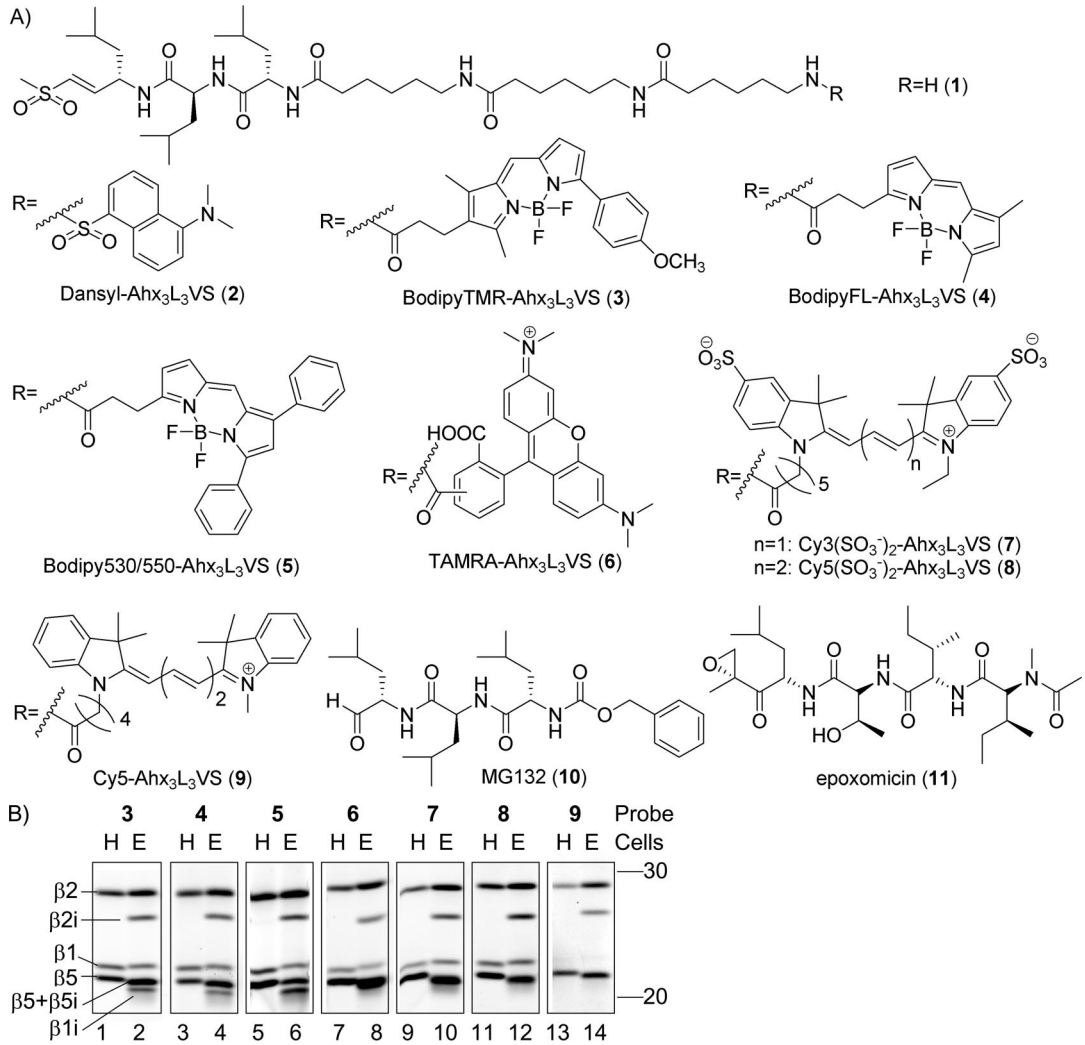

Figure 1. Probes provide an in-gel readout of proteasome subunit availability in cell lysates. (A) All probes are based on structure **1**, which contains a reactive vinylsulfone part (VS) coupled to three leucine residues (L_3) and a spacer consisting of three aminohexanoic acid moieties (Ahx_3). A dansyl moiety or different fluorophores can be coupled to this inhibitory segment, yielding the dansyl probe **2** and benchmark **3** described previously[14,19] as well as probes **4**–**9** used here. (B) Representative gel images showing results of a labeling experiment with 500 nM probes **3**–**9** (1 h) in HeLa and EL4 cell lysates. Proteins were separated using a 12.5%, 20 cm SDS–PAGE gel, affording separation of most subunits in a one-dimensional SDS–PAGE format. Filter settings, exposure time, and image contrast settings were optimized for each individual probe. H = HeLa lysate; E = EL-4 lysate, and i = immunoproteasome subunit.

samples, and the method should be applicable to patient material, allowing tumor profiling, which is likely to improve responses to proteasome inhibitor therapy. For these reasons, we embarked on the synthesis of a range of fluorescent inhibitors so we would be able to select for effective fluorescent proteasome inhibitors with good biochemical and biophysical properties. We furthermore describe the full validation of all probes described; we report the development of procedures that distinguish live cell labeling events from in vitro postlysis artifacts, and we have extended the live cell labeling procedures into flow cytometry-based assays. The latter approach could alter diagnostic means for (overall) proteasome activities and susceptibility to inhibition since it allows for significant throughputs using minimal amounts of material.

Results and Discussion

Probe Preparation and Characterization in Cell Lysates. All probes were based on an $H_2NAhx_3L_3VS$ inhibitory segment (**1**) (Figure 1A) and functionalized with different types of fluorophores. Since different fluorophores possess different biophysical properties, such as membrane permeability, a library of fluorescent proteasome probes was synthesized (see the Supporting Information and Figure 1 therein for experimental procedures). The following probes were selected for further investigation: BodipyFL-Ahx_3L_3VS (**4**), Bodipy530/550-Ahx_3L_3VS (**5**), TAMRA-Ahx_3L_3VS (**6**), Cy3$(SO_3^-)_2$-Ahx_3L_3VS (**7**), Cy5$(SO_3^-)_2$-Ahx_3L_3VS (**8**), and Cy5-Ahx_3L_3VS (**9**). They were compared to the control probe BodipyTMR-Ahx_3L_3VS (**3**) (Figure 1A) about which we recently communicated our findings.[14] These probes span a

large emission spectrum, ranging from green (**4**, $\lambda_{em} \approx 510$ nm) to orange/red (**3** and **5**–**7**, $\lambda_{em} \approx 590$ nm) and far red (**8** and **9**, $\lambda_{em} \approx 670$ nm), which makes it possible to combine them with other fluorescent biomolecules (such as GFP and RFP) and with each other in pulse–chase experiments.

The ability of these probes to provide an in-gel readout of proteasome subunit availability was investigated (Figure 1B). Lysates from both HeLa cells (human, cervix carcinoma) and EL4 cells (murine thymoma) were incubated with probes **3**–**9**. Proteins were separated by SDS–PAGE, and the wet gel slab was directly scanned using a fluorescence scanner with appropriate filter settings. As shown in Figure 1B, probes **3**–**9** labeled a distinct set of proteins in both HeLa and EL4 cell lysates. These proteins could be specifically immunoprecipitated using antiproteasome antibodies (data not shown) and identified as the indicated proteasome active subunits on the basis of the labeling patterns found with probe **2**, the identities of which we recently confirmed by mass spectrometry.[21] Nonspecific labeling in high-molecular weight regions was not observed (Figure 2 of the Supporting Information), suggesting that these probes are specific for proteasomes in cell lysates at the concentrations used.

The different fluorescent moieties were found to affect the fine specificities of individual probes. Both benchmark **3** and bodipy FL-labeled probe **4** afforded quite uniform labeling patterns (Figure 1B, lanes 1–4), suggesting that these probes have similar affinities for all catalytically active subunits. The other probes exhibited enhanced reactivity toward particular subunits (Figure 1B, lanes 5–14). In HeLa cells, probes **5**–**9** labeled the β5 subunit more efficiently than the β1 and β2 subunits. In addition, probe **6** and in particular probe **9** poorly labeled β1 subunits. Furthermore, Figure 1B shows that most subunits labeled with probes **3**–**5** can be resolved by one-dimensional SDS–PAGE. Subunits labeled with probes **6**–**9** are more difficult to separate with good resolution. This suggests that Bodipy-labeled probes allow easier interpretation of complex labeling patterns. Altogether, results indicate that all probes give an in-gel readout that correlates with proteasome activity. Nonetheless, probes **3** and **4** are preferred for in-gel readouts.

Proteasome Labeling in Living Cells. To study which probes can be used to probe living cells, flow cytometry experiments were performed. MelJuSo cells (human melanoma) were incubated with individual probes, and fluorescence intensity was measured. Figure 3 of the Supporting Information shows that benchmark **3** as well as probes **4**–**6** and **9** accumulated in living cells. Probes **7** and **8** on the other hand were not taken up by these cells and were therefore not subjected to further studies, but may be used in experiments on cell lysates.

Proteasome inhibition by **3**–**6** and **9** in living cells was studied, using MelJuSo cells stably expressing ubiquitin-R-GFP (Ub-R-GFP).[15] Following the N-end rule, Ub-R-GFP is rapidly degraded by the proteasome under steady state conditions. Upon inhibition of the proteasome, the GFP concentration in the cells will increase over time, which can be quantified by flow cytometry. Cells were incubated with probe or the general proteasome inhibitor MG132 (ZL_3CHO, **10**). The percentage of cells responding to MG132 was taken to be 100%, and GFP induction in other samples was normalized accordingly. Since the fluorescence emitted by **4** is comparable in wavelength to GFP fluorescence (λ_{ex} and λ_{em} = 480 and 530 nm, respectively), nontransfected MelJuSo cells incubated with this probe were used to normalize the signal (Figure 4 of the Supporting Information). Figure 2A shows that cellular accumulation did not necessarily result in proteasome binding and inhibition. Only probes **3** and **4** induced substantial GFP fluorescence, confirming that only these two compounds efficiently inhibit proteasomes in cultured cells.

Confocal laser scanning microscopy (CLSM) allows us to study probe localization in living cells, as demonstrated previously.[14] To validate that probes **5**, **6**, and **9** accumulate in the cells but do not bind the proteasome, MelJuSo cells were incubated and imaged. Figure 2B shows that probe **5** was mainly visible in granular structures near the nucleus. Probes **6** and **9**, both lipophilic and cationic probes (Figure 1A), were found to accumulate in mitochondria, as visualized by colocalization with MitoTracker green (Figure 2B), and remained there for extended periods of time. Lipophilic cations are often found to accumulate in mitochondria due to the mitochondrial membrane potential.[22] Upon fixation with formaldehyde, **6** and **9** gave a distribution similar to that observed for GFP-labeled proteasomes,[23] indicating that these probes are not covalently bound to mitochondria but merely accumulate there (Figure 5 of the Supporting Information).

To study colocalization of proteasomes with benchmark **3** and probe **4**, both of which inhibited proteasomes in living cells, MelJuSo cells that stably expressed either β1i-GFP[23] or β7-red fluorescent protein (RFP) were incubated with individual probes, washed to remove excess probe, and imaged by CLSM. As shown in Figure 2C, GFP- and RFP-labeled proteasomes were distributed uniformly throughout the nucleus and cytoplasm, with the exception of nucleoli, the nuclear envelope, and the ER/Golgi, consistent with previous reports.[14,23] Compound **3** afforded a similar distribution, as reported,[14] as did compound **4**, and the overlays of proteasome and probe signals revealed substantial colocalization of both probes with GFP- and RFP-labeled proteasomes. Non-colocalizing, free probe could be observed in vesicular structures (Figure 2C), which are likely to be endosomes, since lipophilicity and high molecular weight

(21) Kraus, M.; Ruckrich, T.; Reich, M.; Gogel, J.; Beck, A.; Kammer, W.; Berkers, C. R.; Burg, D.; Overkleeft, H.; Ovaa, H.; Driessen, C. Activity patterns of proteasome subunits reflect bortezomib sensitivity of hematologic malignancies and are variable in primary human leukemia cells. *Leukemia* **2007**, *21*, 84–92.

(22) Murphy, M. P.; Smith, R. A. Drug delivery to mitochondria: The key to mitochondrial medicine. *Adv. Drug Delivery Rev.* **2000**, *41*, 235–250.

(23) Reits, E. A.; Benham, A. M.; Plougastel, B.; Neefjes, J.; Trowsdale, J. Dynamics of proteasome distribution in living cells. *EMBO J.* **1997**, *16*, 6087–6094.

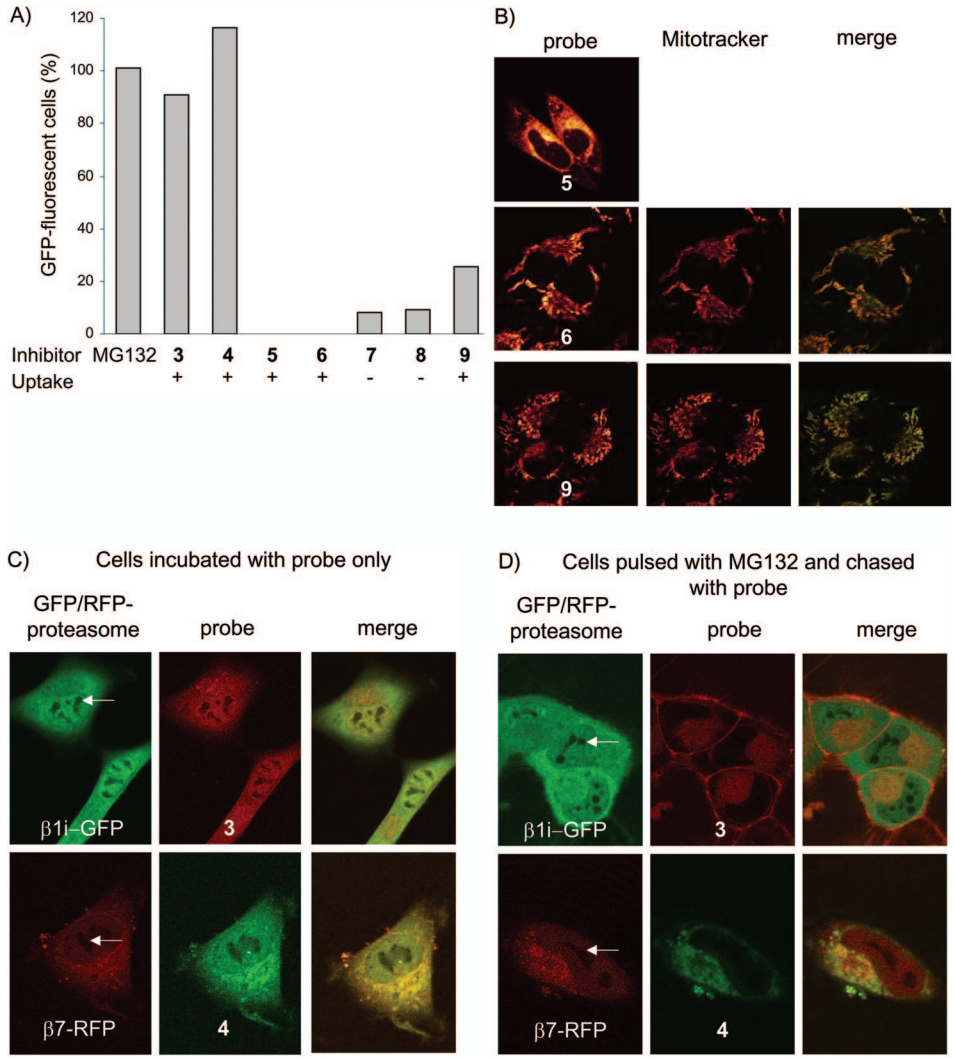

Figure 2. Probes **3** and **4** can be used to study the distribution and activity of proteasomes in living cells. (A) Flow cytometry analysis results of Ub-R-GFP-expressing MelJuSo cells upon incubation with probes **3**–**9** (500 nM) or MG132 (5 μM). The percentage of cells responding to MG132 was taken to be 100%. (B) CLSM images showing MelJuSo cells, incubated with probe **5**, **6**, or **9** (500 nM, 1 h). Cells incubated with **6** or **9** were coincubated with MitoTracker (200 nM, 30 min). From left to right, distribution of probe, localization of MitoTracker, overlay. (C) CLSM images showing MelJuSo cells expressing β7-RFP or β1i-GFP incubated with probe **3** or **4** (1 h). From left to right: localization of GFP- and RFP-labeled proteasome subunits, localization of probe, overlay showing colocalization of probe and proteasome. (D) CLSM images showing MelJuSo cells expressing β7-RFP or β1i-GFP pulsed with MG132 (1 h) and chased with probe **3** or **4** (1 h). From left to right: localization of GFP- and RFP-labeled proteasome subunits after MG132 treatment, localization of probe after MG132 treatment, overlay. Arrows indicate unstained nucleoli.

are factors known to promote uptake via the endosomal pathway.[24] To verify the actual labeling of proteasomes in this experiment, cells were treated as described and lysed and proteins resolved by SDS–PAGE (Figure 6 of the Supporting Information). A clean proteasome labeling pattern was obtained, confirming that at least part of the colocalizing probe is proteasome-bound.

To further study whether all colocalizing probe is proteasome-bound, cells were pulsed with MG132, washed, and chased with either benchmark **3** or probe **4**. Figure 2D (merge) reveals that under these conditions, probes no longer colocalized with GFP- and RFP-labeled proteasomes. This effect could be visualized best in nuclei, which can be recognized from their unstained nucleoli. Instead, probe that was taken up by the cells now remained confined to the plasma membrane and the perinuclear area as free probe. MG132 treatment is reported to block all catalytic sites of the proteasome,[25] preventing probe binding. Since inhibition with MG132 can only alter the intracellular distribution of proteasome-bound probe, but not of free probe, it provides a reliable method for controlling for nonspecific interactions

(24) Lipinski, C. A.; Lombardo, F.; Dominy, B. W.; Feeney, P. J. Experimental and computational approaches to estimate solubility and permeability in drug discovery and development settings. *Adv. Drug Delivery Rev.* **2001**, *46*, 3–26.

(25) Kisselev, A. F.; Goldberg, A. L. Proteasome inhibitors: From research tools to drug candidates. *Chem. Biol.* **2001**, *8*, 739–758.

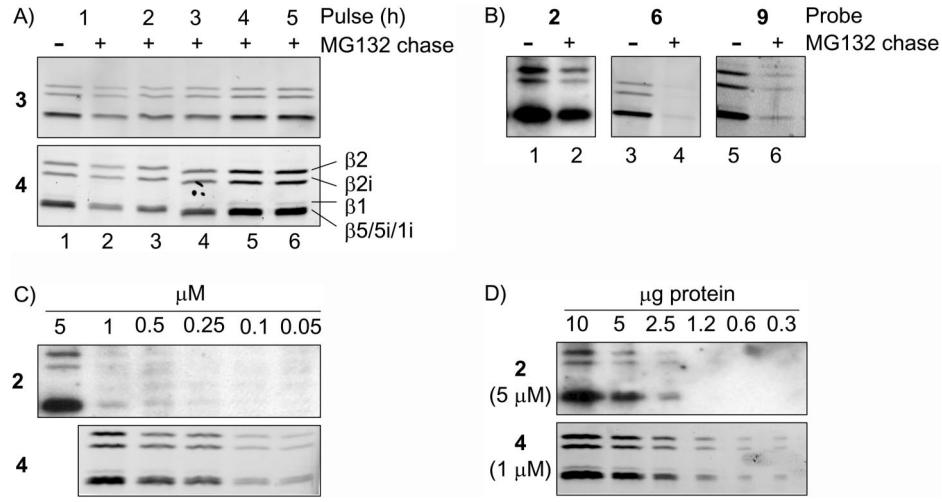

Figure 3. Probes **3** and **4** function as highly sensitive proteasome subunit activity reporters in living cells. (A and B) Gel images and immunoblot showing proteasome labeling in living EL4 cells that were pulsed with probe **3** or **4** (375 nM, indicated times) (A) or with probes **6** and **9** (375 nM, 1 h) or **2** (5 μM, 2 h) (B) and either harvested directly or chased with 5 μM MG132 (1 h). (C and D) Gel image and immunoblot showing proteasome labeling in living EL4 cells, incubated with probe **2** or **4** (2 h), with either increasing probe concentrations (C) or increasing levels of protein loading on gel (D). Proteins were separated using mini-gels (that do not separate the β1i subunit from the β5 subunits).

of probes **3** and **4**. Figure 6 of the Supporting Information shows that MG132 treatment resulted in 85–94% block of proteasome labeling. Labeling of additional proteases was not observed, suggesting that only free probe was left in the cells after MG132 treatment. These results suggest that the signal observed in cytosol and nucleus in Figure 2C can fully be attributed to proteasome-bound probe and that probes **3** and **4** can be used to study proteasome distribution and profile the activity of proteasomes in living cells.

Optimization of In-Gel Activity Assay in Living Cells. Next, we set out to optimize the gel assay described above. In CLSM experiments, some residual free probe **3** and **4** was observed in membrane structures (Figure 2C). Since cells have to be lysed for a gel-based readout, internal membrane structures are destroyed, which may release unbound probe. This potentially results in additional labeling, disturbing the accuracy of readouts. To prevent postlysis labeling, cells were pulsed with either probe **3** or **4** for various periods of time and chased with MG132 to block residual catalytic sites (Figure 3A, lanes 2–6). To show the contribution of postlysis labeling, cells were pulsed for 1 h and harvested directly (Figure 3A, lane 1). Proteins were separated using a mini-gel system, which does not separate the β1i, β5, and β5i subunits from each other, explaining the slightly different labeling patterns in Figure 3 compared to Figure 1B. A 1 h pulse with **3** or **4** followed by a MG132 chase revealed substantial proteasome labeling (Figure 3A, lane 2). Labeling intensities increased with incubation time and were saturated at an incubation time of 4 h. Since the relative labeling patterns did not change (Figure 3A, lanes 3–6), the 1 h labeling period (Figure 3A, lane 2) was sufficient to obtain a representative proteasome labeling profile. When samples were not chased, additional labeling could be observed (in Figure 3A, compare lanes 1 and 2), suggesting that postlysis artifacts are likely to occur.

To verify that this procedure ensures a proper live cell readout, the experiment was repeated with probe **2**, which should afford a live cell readout,[19] and with probes **6** and **9**, which localize to the mitochondria and should therefore barely label proteasomes in living cells. Cells were pulsed with probes **2**, **6**, and **9** and either chased with MG132 or harvested directly. When probe **2** was used,[19] the results were similar to those observed with probes **3** and **4** (Figure 3B, lanes 1 and 2). The MG132 chase completely abolished labeling using probes **6** and **9** (Figure 3B, lanes 4 and 6). Without an MG132 chase, on the other hand, both probes afforded proteasome labeling (Figure 3B, lanes 3 and 5). These observations confirm the validity of the method applied and are a warning for postlysis labeling that can be mistaken for a genuine live cell labeling event. It is, therefore, important to chase with a nonfluorescent pan-proteasome inhibitor like MG132, to ensure a correct interpretation of the results.

Fluorescent Probe 4 versus Dansylated Probe 2. Having optimized the in-gel activity assay as described above, we compared dansylated probe **2** to fluorescent probe **4**. EL4 cells were pulsed with various concentrations of probe **2** or **4**, followed by a MG132 chase. Figure 3C shows that for a clear and equal visualization of all subunits, cells needed to be incubated with 5 μM **2**, while 50 nM **4** was sufficient. To confirm these data, EL4 cells were pulsed with probe **2** or **4** and chased with MG132, after which different amounts of total lysate were analyzed by SDS–PAGE. As seen in Figure 3D, 300 ng of total lysate was sufficient for proteasome visualization when probe **4** was used. Although cells were incubated with a 5-fold molar excess of probe **2** (5

μM) compared to probe **4** (1 μM), 2.5 μg of total lysate was needed to generate sufficient signal using probe **2**. From these results, it can be concluded that when living cells are probed for proteasome activity using the pulse–chase procedure described here, fluorescent probe **4** affords an up to 100-fold improvement in sensitivity compared to the dansylated probe **2** described previously and properties comparable to that of **3**, in principle allowing bioorthogonal use of multiple probes.

Profiling Mouse Tissues. Several methods have been used to study the bioavailability of proteasome inhibitors (see above).[17,18] However, sensitive methods that can be used to study the in vivo subunit-specific activity of proteasome inhibitors are in great demand. In our previous setup, probe was injected into the mouse, after which organs could be imaged and analyzed.[14] This setup is, however, not suitable for studying proteasome activity in patient material or in tissues where these probes may not accumulate sufficiently. We therefore employed an ex vivo approach, using probe **4** to identify the tissue-specific activity of the different catalytic β-subunits of proteasomes in freshly isolated organs. To determine whether probe **4** was effectively taken up in different cell types, segments of different organs were incubated with **4** (Figure 4A). Due to the complex nature of tissues (e.g., muscle cells in the heart), nuclear staining (DAPI) was used as counter stain (Figure 7 of the Supporting Information). Images were obtained by sequential scanning, and autofluorescence was found to be minimal (Figure 7 of the Supporting Information). Figure 4A shows that probe **4** was taken up by all cell types.

Next, we profiled proteasome activity in this panel of mouse tissues (Figure 4B). To this end, single-cell suspensions were obtained and red blood cells lysed. Cells were pulsed with compound **4** and chased with MG132. Samples were normalized to either cell number or protein content without observing significant differences in the results that were obtained. Band intensities were quantified and plotted as a percentage of the total proteasome labeling intensity (Figure 4B, bottom panel). A great variation in subunit-specific labeling was observed, depending on the organ that was probed (Figure 4B). Substantial labeling of immunoproteasome subunits was found in lymphoid organs (Figure 4B, lanes 1, 2, and 5). Immunoproteasome subunits could also be detected in lung tissue (Figure 4B, lane 3), although at lower intensities. In brain, liver, heart, and kidney tissue (Figure 4B, lanes 4 and 6–8), active immunoproteasome subunits could not be detected. Immunoproteasome expression favors the production of antigenic peptides for MHC class I antigen presentation, and high-level immunoproteasome expression has been reported for lymphoid organs (spleen, lymph nodes, and thymus),[6] correlating with the immunoproteasome labeling by **4**. Thus, probe **4** seems well suited to visualization of immunoproteasome regulation.

Next to the presence of immunoproteasome subunits, an additional level of proteasomal activity regulation appeared visible. Although equal amounts of subunits β1, β2, and β5 are thought to be incorporated in functional proteasomes, different labeling intensities were observed in different tissues (Figure 4B), in line with the existence of different proteasome subtypes.[7,8] In lung and thymus, all subunits contributed equally to the total proteasome activity (Figure 4B, lanes 3 and 5). In brain, β2 and β5 subunits were labeled with the greatest intensity (Figure 4B, lane 4), while mainly β1 and β2 subunit labeling was observed in spleen and lymph nodes (Figure 4B, lanes 1 and 2). In the liver, kidney, and heart (Figure 4B, lanes 6–8), β2 subunits were most intensely labeled. These results indicate that different cell types display different ratios of proteasomal activities, suggesting that subunit activity is regulated in an organ-specific manner. This may influence substrate degradation, as well as the response to proteasome inhibitors. Probe **4** labeled an additional protein as well, which could not be immunoprecipitated with an antibody raised against the 20S proteasome (data not shown). Labeling in spleen tissue could be abolished by preincubation with MG132 (Figure 4C), which is known to inhibit cathepsins.[25] In H929 cells (human, multiple myeloma) and in spleen cell lysates, labeling was abolished by both the pan-cathepsin inhibitors LHVS[26,27] and JPM-565[28,29] (Figure 8 of the Supporting Information), suggesting that this band represents a cathepsin.

To validate whether an ex vivo approach would allow profiling of the pharmacodynamics of proteasome inhibitors in intact organs, intact tissue segments of spleen and thymus were incubated with different concentrations of MG132 and the broad-spectrum proteasome inhibitor epoxomicin (**11**) and chased with probe **4** (Figure 4C). Intact tissue segments were less sensitive to proteasome inhibitors, compared to single-cell suspensions. In the latter, 5 μM MG132 or 1 μM epoxomicin was sufficient to inhibit 90% of the proteasomal activity (Figure 9 of the Supporting Information). In intact tissue segments, on the other hand, 25 μM MG132 and 10 μM epoxomicin did not fully inhibit all proteasomal activities (Figure 4C). These results stress the importance of methods that can profile the in vivo inhibitory action of proteasome inhibitors. The specificity of both proteasome inhibitors in intact tissue segments could be profiled with ease. While MG132 exhibited a preference for the β5 and β1 subunits at low concentrations, as described previously,[19] epoxomicin inhibited all subunits with equal affinity.[30] Furthermore,

(26) Palmer, J. T.; Rasnick, D.; Klaus, J. L.; Bromme, D. Vinyl sulfones as mechanism-based cysteine protease inhibitors. *J. Med. Chem.* **1995**, *38*, 3193–3196.

(27) Riese, R. J.; Wolf, P. R.; Bromme, D.; Natkin, L. R.; Villadangos, J. A.; Ploegh, H. L.; Chapman, H. A. Essential role for cathepsin S in MHC class II-associated invariant chain processing and peptide loading. *Immunity* **1996**, *4*, 357–366.

(28) Meara, J. P.; Rich, D. H. Mechanistic studies on the inactivation of papain by epoxysuccinyl inhibitors. *J. Med. Chem.* **1996**, *39*, 3357–3366.

(29) Shi, G. P.; Munger, J. S.; Meara, J. P.; Rich, D. H.; Chapman, H. A. Molecular cloning and expression of human alveolar macrophage cathepsin S, an elastinolytic cysteine protease. *J. Biol. Chem.* **1992**, *267*, 7258–7262.

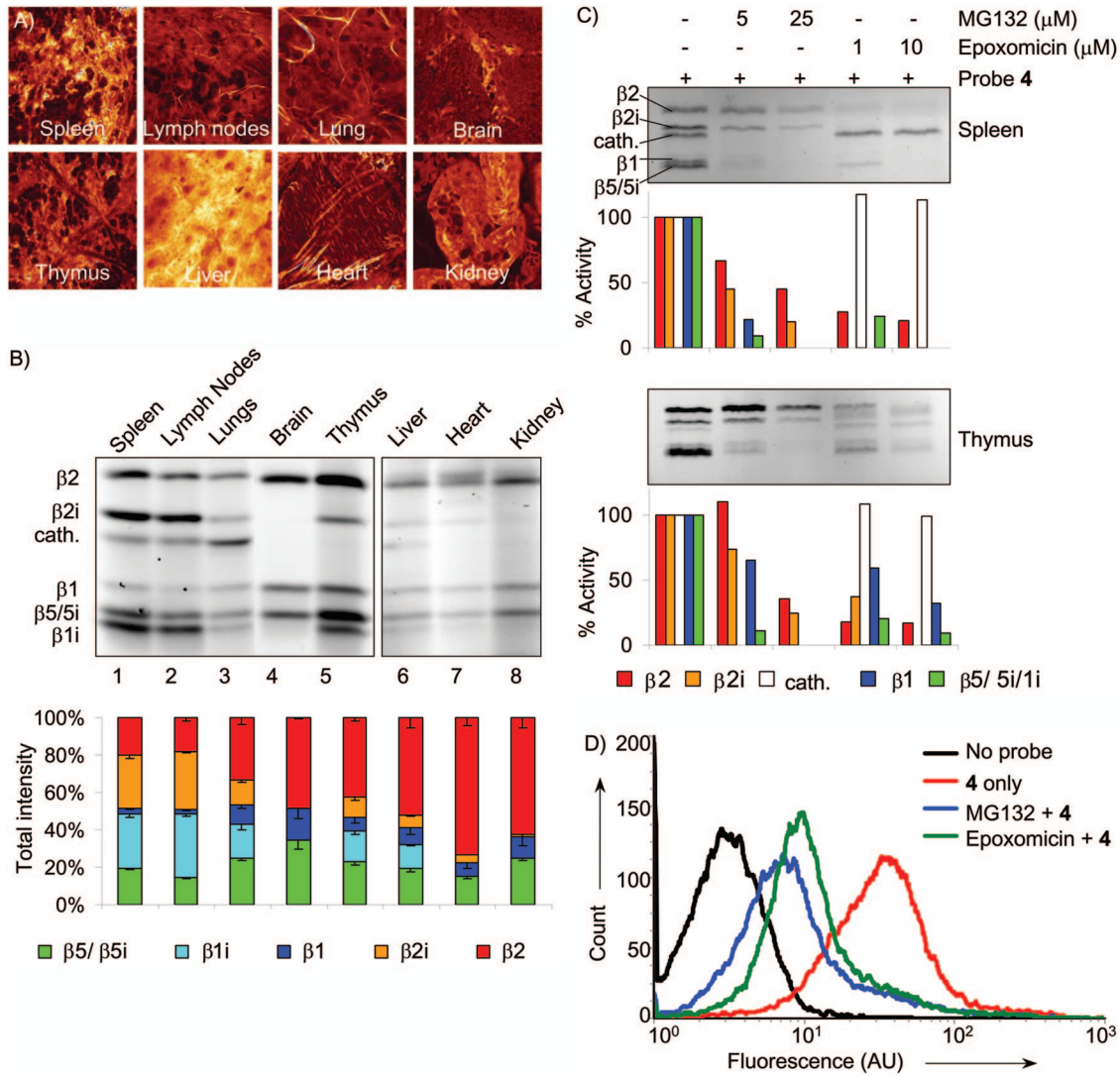

Figure 4. Profiling the proteasome and the effects of proteasome inhibitor treatment in mouse tissues. (A) CLSM images showing whole tissue segments from indicated organs incubated with 500 nM **4** (1 h). (B) Gel image showing active subunit labeling in indicated tissues from mice, pulsed with 500 nM **4** (2 h) and chased with 5 μM MG132 (1 h). Proteins were separated using a 20 cm SDS–PAGE gel to allow separation of β1i and β5 subunits. Because of large differences in absolute labeling intensities between tissues, exposure times and image contrast settings were optimized for lanes 1–5 and 6–8 separately to allow clear visualization of labeled subunits. cath. represents cathepsin (top panel). Plot showing the quantification of band intensities, plotted as a percentage of total proteasome labeling intensity. Values are an average of two independent experiments $\pm$ the standard error of the mean (bottom panel). (C) Gel images showing the active subunit labeling in whole tissue segments from spleen and thymus that were pulsed with the indicated concentrations of MG132 and epoxomicin (1 h) and chased with 500 nM probe **4** (1 h; top panels). Plots showing quantification of band intensities, plotted as a percentage of labeling intensity in untreated tissue (bottom panels). (D) Flow cytometry plots showing the fluorescence in mouse lymphocytes that were not incubated (black), incubated for 1 h with 50 nM **4** (red), or pulsed for 1 h with 1 μM epoxomicin (green) or 5 μM MG132 (blue) and chased with 50 nM **4** (1 h).

MG132 inhibited not only the proteasomal subunits but also a cathepsin,[25] while epoxomicin was highly specific for the proteasome[30] (Figure 4C). To study whether these results could be confirmed by flow cytometry experiments, single-cell suspensions obtained from spleen tissue were pulsed with proteasome inhibitor and chased with **4**, or incubated with **4** alone. Cells were washed, and fluorescence was measured. As seen in Figure 4D, both inhibitors induced a substantial shift in intracellular fluorescence, indicating proteasome inhibition.

Together, these data indicate that two of the fluorescent probes described here could be used to profile the in vivo

(30) Meng, L.; Mohan, R.; Kwok, B. H.; Elofsson, M.; Sin, N.; Crews, C. M. Epoxomicin, a potent and selective proteasome inhibitor, exhibits in vivo antiinflammatory activity. *Proc. Natl. Acad. Sci. U.S.A.* **1999**, *96*, 10403–10408.

pharmacological properties of proteasome inhibitors, both quantitative, using flow cytometry, and qualitative, using SDS–PAGE readouts to profile distinct proteasomal active subunits. Although our studies have been limited to mouse tissue, the method used should be equally applicable to any other sample, enabling proteasome profiling and competition assays in clinical settings.

Conclusion

We devised a range of fluorescent proteasome activity reporters. Two probes, BodipyTMR-labeled **3**,[14] and BodipyFL-labeled probe **4**, can efficiently bind to all catalytically active subunits of proteasomes in living cells. Other probes described herein may be used for the analysis of cell homogenates. In addition, when probe **4** is compared to previously developed methods for probing proteasome activity in living cells (probe **2**), the newly developed probe is up to 100-fold more sensitive.

Using probe **4**, we set up gel-based and flow cytometry methods to study proteasome activity in living cells and to probe organ-specific proteasome activity. Our results indicate that different tissue types exhibit a different subunit labeling pattern, suggesting that subunit activity is regulated in an organ-specific manner. Furthermore, the tools and methods described here should be well-suited to the performance of pharmacological studies with proteasome inhibitors under clinical evaluation. In addition, the methodology described here should be applicable to monitoring proteasome activity in samples from patients that are treated with proteasome inhibitors.

Materials and Methods

Bodipy and TAMRA dyes were purchased from Invitrogen or Molecular Probes. Sulfated cyanine (Cy3 and Cy5) dyes were purchased from Amersham, whereas the nonsulfated Cy5 analogue was synthesized according to a published procedure.[31] Peptide building blocks were purchased from Novabiochem and appropriately functionalized resins from Applied Biosystems. All solvents were purchased from Biosolve at the highest grade available. All other chemicals were purchased from Aldrich at the highest available purity. All solvents and chemicals were used as received. Liquid chromatography–mass spectroscopy (LC–MS) analyses were carried out on a WATERS LCT mass spectrometer in line with a WATERS 2795 HPLC system and a WATERS 2996 photodiode array detector. Analytical and preparative HPLC runs were performed on a Waters 1525 EF HPLC system coupled to a Waters 2487 dual λ absorbance detector.

Probe Synthesis. See the Supporting Information for detailed information on synthetic procedures and purity analysis.

Cell Culture. EL4 (mouse, thymoma) and H929 (human, multiple myeloma) cells were cultured in RPMI 1640 (Invitrogen). Cell lines HeLa (human, cervix carcinoma) and MelJuSo (human, melanoma) were cultured in DMEM (Invitrogen). MelJuSo cells expressing β1i-GFP,[23] β7-RFP, or Ub-R-GFP[15] were cultured in DMEM in the presence of zeomycin (RFP) and geomycin (GFP) selection. Prior to CLSM imaging, cells were cultured overnight in DMEM lacking phenol red to prevent autofluorescence of the medium. All media were supplemented with 10% fetal calf serum (FCS), 100 units/mL penicillin, and 100 μg/mL streptomycin.

In-Gel Profiling of Proteasomes in Cell Lysates. EL4 and HeLa cells were mechanically lysed using glass beads.[11] To this end, cells were washed with PBS, pelleted, and lysed by being vortexed at high speed at 4 °C for 45 min with 1 volume of glass beads (<106 μm, acid-washed, Sigma) and 1 volume of homogenization buffer [50 mM Tris (pH 7.4), 5 mM $MgCl_2$, 250 mM sucrose, 1 mM DTT, and 2 mM ATP]. Beads, membrane fractions, and cell debris were removed by centrifugation at 16000*g* for 5 min. Protein concentrations were determined using the Bradford assay (Bio-Rad), and 50 μg of protein was incubated with compounds **3**–**9** (500 nM) for 1 h at 37 °C. Proteins were denatured by being boiled in reducing sample buffer and analyzed by 12.5% SDS–PAGE using a PROTEAN II xi Cell system (Bio-Rad).

In-Gel Profiling of Proteasomes in Living Cells. MelJuSo cells were incubated with 500 nM probe **3** or **4** or pulsed with 5 μM MG132 and chased with 500 nM **3** or **4**, both followed by a wash step. EL4 cells (1×10^6) in 1 mL of RPMI were incubated with 375 nM compound **3** or **4** for 1–5 h, 375 nM probe **6** or **9** for 1 h, or 5 μM **2** for 2 h, followed by a 1 h chase with 5 μM MG132. Control samples were incubated with 375 nM probe **3**, **4**, **6**, or **9** alone for 1 h or with 5 μM **2** alone for 2 h. Cells were harvested and lysed for 30 min in NP40 lysis buffer [50 mM Tris (pH 7.4), 150 mM NaCl, and 1% NP40] at 4 °C. The Bradford assay was used to measure protein content. For experiments using cathepsin inhibitors, H929 cells were incubated with 500 nM **4** (1 h) or pulsed with 10 or 50 μM LHVS or JPM-565 (1 h) and chased with 500 nM **4** (1 h). Cells were lysed in NP40 lysis buffer as described above.

Comparison between Dansylated and Fluorescent Proteasome Probes. EL4 cells (1×10^6/mL) were pulsed for 2 h with the indicated (Figure 4C) concentrations of probe **2** or **4**, followed by a 1 h chase with 5 μM MG132. Cells were harvested and lysed in NP40 lysis buffer. The Bradford assay was used to measure protein content, and equal amounts of protein were analyzed by 12.5% SDS–PAGE. Alternatively, EL4 cells (1×10^6/mL) were pulsed for 2 h with 5 μM **2** or 1 μM **4**, and chased with MG132 (5 μM, 1 h). Cells were lysed in NP40 lysis buffer, and protein content was determined as described above.

Mouse Tissue Analysis by SDS–PAGE. C57BL/6 mice were bred under pathogen-free conditions according to national and institutional guidelines and were sacrificed at 6–10 weeks of age. Subsequently, spleen, lymph nodes, lungs, liver, heart, kidneys, brain, and thymus were isolated. Single-cell suspensions were made using 70 μm nylon cell

(31) Korbel, G. A.; Lalic, G.; Shair, M. D. Reaction microarrays: A method for rapidly determining the enantiomeric excess of thousands of samples. *J. Am. Chem. Soc.* **2001**, *123*, 361–362.

strainers (BD Biosciences). Heart tissue was pretreated with 1 mg/mL collagenase V (Sigma) and 1% DNase I (Ambion) for 30 min at 37 °C before single-cell suspensions were obtained. Red blood cells were lysed by hypotonic lysis, and cells were resuspended at a density of 5×10^6 cells/mL. Cells were incubated for 2 h with 500 nM **4**, followed by a 1 h chase with 5 μM MG132 to block postlysis labeling. Cells were harvested and lysed for 30 min at 4 °C using NP40 lysis buffer. Protein concentrations were determined using the Bradford assay. Lysate from 1×10^6 cells or equal amounts of protein were denatured by being boiled in reducing sample buffer, and polypeptides were analyzed by 12.5% SDS–PAGE using a PROTEAN II xi Cell system (Bio-Rad). To assess the effect of treatment with different proteasome inhibitors, whole tissue segments of spleen and thymus were placed in 1 mL of DMEM. In addition, a single-cell suspension was obtained from thymus (5×10^6 cells/mL). Tissue segments and single-cell suspensions were pulsed with MG132 (5 and 25 μM), epoxomicin (1 and 10 μM), or DMSO (1 h, 37 °C), chased with 500 nM **4** (1 h, 37 °C), and washed with fresh DMEM (1 h, 37 °C). Cells and tissue segments were lysed at 4 °C using NP40 lysis buffer. Protein concentrations were determined using the Bradford assay. Equal amounts of protein were denatured by being boiled in reducing sample buffer, and polypeptides were analyzed by 12.5% SDS–PAGE using a mini-gel system (Bio-Rad). For experiments using cathepsin inhibitors, spleen cells were lysed mechanically as described above. Equal amounts of protein were either incubated with 1 μM probe **4** (1 h) or pulsed with 10 or 50 μM LHVS or JPM-565 (1 h) and chased with 1 μM **4** (1 h).

In-Gel Fluorescence Measurements. Proteins were denatured by being boiled in reducing sample buffer and analyzed by 12.5% SDS–PAGE. Wet gel slabs were imaged for 2 min, with a resolution of 100 μm, using a ProXPRESS 2D Proteomic imaging system (Perkin Elmer), using the following filter settings: probe **4**, λ_{ex} and $\lambda_{em} = 480$ and 530, respectively; probes **3** and **5–7**, λ_{ex} and $\lambda_{em} = 550$ and 590 nm, respectively; and probes **8** and **9**, λ_{ex} and $\lambda_{em} = 625$ and 680 nm, respectively. Images were analyzed using Totallab analysis software (Nonlinear Dynamics, Newcastle upon Tyne, U.K.).

Assaying Proteasome Activity by Immunoblotting (probe 2). Proteins were denatured by being boiled in reducing sample buffer and separated by 12.5% SDS–PAGE gel followed by electro-transfer onto PVDF membranes. Immunoblotting was performed using an antidansyl-sulfonamidohexanoyl polyclonal Ab (1:1000, rabbit, Molecular Probes) and HRP-coupled swine anti-rabbit secondary antibody (DAKO) followed by enhanced chemiluminescence (SuperSignal West Dura Extended Duration, Pierce).

Flow Cytometry Experiments. Flow cytometry experiments were performed on a FACSCalibur 2 apparatus (BD Biosciences). For uptake experiments, MelJuSo cells were incubated with 500 nM probes **3–9** for 1 h. Cells were washed, trypsinized, and resuspended in medium, and intracellular fluorescence was measured. For inhibition experiments in cultured cells, both MelJuSo cells (control) and MelJuSo cells stably expressing a Ub-R-GFP construct were incubated with 500 nM probes **3–9** for 12 h. Cells were washed, trypsinized, and resuspended in medium. Subsequently, GFP fluorescence was measured. As a control for Ub-R-GFP expression, cells were incubated with 5 μM MG132 for 1.5 h, followed by analysis of GFP fluorescence. Since the fluorescence emitted by **4** is comparable in wavelength to GFP fluorescence (λ_{ex} and $\lambda_{em} = 480$ and 530 nm, respectively), nonengineered MelJuSo cells incubated with this probe were used to normalize the signal. For inhibition experiments in mouse tissue, a single-cell suspension from mouse spleen was obtained (see above). Samples were pulsed with either MG132 (5 μM) or epoxomicin (1 μM) for 1 h at 37 °C and chased with 50 nM **4** for 1 h at 37 °C. As a control, cells were incubated with **4** alone or not incubated. Cells were washed three times with fresh DMEM for 20 min at 37 °C. Subsequently, intracellular fluorescence was measured.

CLSM Imaging of Cultured Cells. CLSM images were recorded using a Leica-SP2 system connected to an inverted microscope (Leica DM IR/E 2) and a tissue culture box at 37 °C. MelJuSo cells expressing β7-RFP or β1i-GFP were incubated for 1 h with 500 nM **3**, **4**, or **5**. Cells were washed with medium before being imaged. For the pulse–chase studies, MelJuSo cells expressing β1i-GFP or β7-RFP were incubated for 1 h with 5 μM MG132, washed with medium, and chased for 1 h with 500 nM **3** or **4**, respectively. To study probe **6** or **9**, MelJuSo cells were incubated for 1 h with either probe (500 nM) and washed. To visualize mitochondria, 200 nM MitoTracker green (Invitrogen) was added (30 min), and the cells were washed.

CLSM Imaging of Tissue Slices. CLSM images were recorded using a Leica-SP2 AOBS system connected to an inverted microscope (Leica DM IR/E 2) and a tissue culture box at 37 °C with 5% CO_2. All images were obtained by sequential scanning and with identical settings. Spleen, lymph nodes, lungs, liver, heart, kidneys, brain, and thymus were isolated from C57BL/6 mice and sliced into small segments (±0.5 mm thick). Tissue segments were placed in 1 mL of DMEM and incubated with 500 nM **4** and 2×10^{-3} mg/mL DAPI. After incubation, the wet segment was placed on a glass coverslip with a drop of fresh medium, covered by a secondary coverslip, and imaged. To obtain autofluorescence images, tissue segments were not incubated, but directly imaged using identical settings.

Acknowledgment. We thank Henk Hilkmann for assistance with automated peptide synthesis, Dr. Christoph Lippuner for technical assistance, and Dr. Danny Burg for in-depth discussions. This work was funded by the Dutch Cancer Society, Project Grant NKI 2005-3368.

Supporting Information Available: Additional experimental details and results. This material is available free of charge via the Internet at http://pubs.acs.org.

MP0700256